Institutionen för systemteknik
Department of Electrical Engineering

Examensarbete

Controlled Start Transmission Wet Clutch Temperature Modeling and Application

Examensarbete utfört i Fordonssystem
vid Tekniska högskolan vid Linköpings universitet
av

Joel Martinsson

LiTH-ISY-EX--15/4895--SE

Linköping 2015

Linköpings universitet
TEKNISKA HÖGSKOLAN

Department of Electrical Engineering
Linköpings universitet
SE-581 83 Linköping, Sweden

Linköpings tekniska högskola
Linköpings universitet
581 83 Linköping

Controlled Start Transmission Wet Clutch Temperature Modeling and Application

Examensarbete utfört i Fordonssystem
vid Tekniska högskolan vid Linköpings universitet
av

Joel Martinsson

LiTH-ISY-EX--15/4895--SE

Handledare:	**Vaheed Nezhadali**
	ɪsy, Linköpings universitet
	Bin Liu
	ABB Corporate Research
Examinator:	**Lars Eriksson**
	ɪsy, Linköpings universitet

Linköping, 12 oktober 2015

| | |

Titel
Title   Controlled Start Transmission Wet Clutch Temperature Modeling and Application

Författare   Joel Martinsson
Author

Sammanfattning
Abstract

    Controlled Start Transmissions (CST) can be described as a mechanical transmission combined with a wet clutch for controlled torque output. CST:s are commonly used to start up heavy loads for example mining conveyors. Several CST:s can work together to share the load. The transferred torque is controlled by a hydraulic wet clutch which is a proven technology for high torque transfer and low wear. This thesis is a part of a project to increase the knowledge and improve the CST design and control performance. The heat generation in the wet clutch is the focus of this thesis. Literature review shows that most research is done in order to get high accuracy for smaller clutches and most of the high torque engagements have very short transients. Models for the CST clutch heat generation together with thermal behavior have been developed and investigated. This includes a temperature model together with a kinetic model of the gearbox and a clutch torque model. Validation of separate model components and sensitivity analysis of the parameters are made. The developed model is then analyzed by comparing measurements from a commission site and simulations to get an idea of how much heat is generated.

Nyckelord
Keywords   Wet clutch, Modeling, Controlled Start Transmission, Temperature

Abstract

Controlled Start Transmissions (CST) can be described as a mechanical transmission combined with a wet clutch for controlled torque output. CST:s are commonly used to start up heavy loads for example mining conveyors. Several CST:s can work together to share the load. The transferred torque is controlled by a hydraulic wet clutch which is a proven technology for high torque transfer and low wear. This thesis is a part of a project to increase the knowledge and improve the CST design and control performance. The heat generation in the wet clutch is the focus of this thesis. Literature review shows that most research is done in order to get high accuracy for smaller clutches and most of the high torque engagements have very short transients. Models for the CST clutch heat generation together with thermal behavior have been developed and investigated. This includes a temperature model together with a kinetic model of the gearbox and a clutch torque model. Validation of separate model components and sensitivity analysis of the parameters are made. The developed model is then analyzed by comparing measurements from a commission site and simulations to get an idea of how much heat is generated.

Acknowledgments

I would like to thank ABB and all of the people I was meeting during this time in Västerås. Especially I wanted to thank my supervisor Bin Liu for giving me the opportunity to do my thesis at ABB and all of the discussions during this time. Moreover I also want to thank my supervisor Vaheed Nezhadali. Finally I want to thank my friends, family and my girlfriend for the support and memories during these intense years, making them a period of my life which I will never forget.

Linköping, September 2015
Joel Martinsson

Contents

Notation

NOTATION

Notation	Meaning
A_{clutch}	Clutch area
A_{pist}	Clutch piston area
β_v	Viscous friction coefficient
C_1 & C_2	Friction coefficients
C_p	Heat capacity for the separator discs
CFD	Computational Fluid Dynamics
CST	Control Start Transmission
d_{SD}	Thickness of separator disc
F_{spring}	The force from the return spring
F_{app}	The force applied to the clutch disc surfaces
HTC	Generalized heat transfer coefficient
M_p	Mass of a single separator disc
N_f	Number of friction surfaces
$N_{fr,discs}$	Number of friction discs
$N_{sp,discs}$	Number of separator discs
N_R	Number of teeth on the ring gear
N_S	Number of teeth on the sun gear
N_C	Total number of teeth on the carrier gear
N_1	Number of teeth for the first input gear
N_2	Number of teeth for the second input gear
$\mu(T)$	Friction coefficient function of temperature
μ_{dyn}	Dynamic viscosity
ν	Kinematic viscosity
ω_{in}	Rotation speed of the electrical motor and input gear.
ω_S	Rotation speed of sun gear
ω_R	Rotation speed of ring gear
ω_C , ω_{load}	Rotation speed of the planet carrier
p	Pressure applied to the clutch
P_{in}	Measured Electrical motor Power
PCV	Proportional Control Valve
PWM	Pulse Width Modulated
PLC	Programmable Logic Controller
ρ_{oil}	Density of hydraulic actuator oil
ρ_{SD}	Density of separator disc
R_e	Effective clutch radius
r_R	Ring radius
r_1	Input gear 1 radius
r_2	Input gear 2 radius

Notation

Notation	Meaning
R_{out}	Outer radius of the clutch
R_{in}	Inner radius of the clutch
R_m	Mean radius
T_{amb}	Ambient temperature
$T_S D$	Temperature of clutch separator disc
τ_{in}	Input torque
$\tau_{in,0}$	Raw measured torque
τ_{comp}	Measured idle torque
τ_{clutch}	Torque transferred through the clutch
$\tau_{visc,max}$	Maximum torque at idle and input gear
V_{SD}	Separator plate volume

1

Introduction

This is a thesis for a Master of Science degree in Applied Physics and Electrical Engineering at Linköping University. The thesis is performed at ABB Corporate Research in Västerås during the spring of 2015 together with the Division of Vehicular Systems, Department of Electrical Engineering at Linköping University.

1.1 Background

Large conveyor systems are often used in mines and other industrial applications and are a cost effective way of transporting large amount of material in long distances. The scale of these conveyor system can be several kilometers long and have heavy loads. When the belt length is long it becomes very difficult to handle the acceleration and the complex dynamics of the belt Romani [2012]. To address this issue, a specific type of mechanical transmission is used, called Controlled Start Transmissions (CST) which can effectively control the transferred torque to the load and ramp the speed by using an integrated wet clutch. However they generate a lot of heat during engagement transients. Other models of the belt and power generation does not describe the thermal behavior and losses of the clutch which is a wanted property to be able to minimize losses and maximize efficiency by investigating simulations.

1.2 Objectives of the thesis

The main objective of the thesis is to construct a model for the hydraulic clutch to include thermodynamic behavior that can later be used to improve system design

and optimize CST design. Another objective is to examine the current system with an approach to system and control performance and look into alternatives for the actuator system. This includes a literature review of current state of the art in hydraulic systems.

1.3   Related Research

In Deur et al. [2005] a static clutch model is experimentally validated to its limits and then expanded to include fluid film dynamics. It is found that a static model is only valid for high initial speed and high rates of change in applied pressure. The resulting model had good fitting and was also expanded with a model for actuator dynamic. This can be a good start for the examination of the actuator system.

In Marklund et al. [2007] a friction model for a Limited Slip Differential (LSD) is developed and verified. This is a good starting point as the speed of a LSD is similar to what is investigated in this thesis. The rotational speed is not so large in revolutions per minute. However, a large radius gives a high surface speed. The application is very small which gives high surface speed and assumptions are made because of this. It is found that temperature has large impact on the torque transferred and requires the friction model to take the temperature into account. This report is later expanded in Marklund and Larsson [2007] presenting an experimental way to estimate the friction parameters using a pin-on-disc measurement in Marklund and Larsson [2008]. This is an alternative to the extensive experimental rigs used in e.g. Ivanović et al. [2009]. Although the result is very good for later usage where such a rig is not available.

In Thornton et al. [2013] a clutch actuator is modeled for control application. The overall purpose is to improve gearshifting in an automatic gearboxes. This is accomplished by combining physical models with system identification in four different region of operation. The goal is to keep the model order low, to make online control possible. It is found that the developed model has good fit for the control purpose.

Applications of LSD temperature models are also available in Seo et al. [2011, 2015], which applies and validates a similar temperature model as this thesis. The measurements and fitting are towards a vehicle mounted LSD. The results shows a positive use for the approach and a good fit to the available measurements.

Overall, this is a well explored field that has been studied for decades though most of the research have its foundation in the automotive industry and around automatic gearboxes with short transients. There is an apparent lack of articles addressing the larger sizes of clutches. This thesis tries to adapt heat transfer models for smaller vehicle clutches onto a large CST clutch. There are methods that can be used for the heat transfer analysis but there is a significant difference in size and torque. In the CST system the clutch surface velocity can be higher

and the torque can be hundreds of kNm.

1.4   Thesis Outline

This thesis is divided into the following chapters:

- Chapter 1 is an introduction to the thesis. Including a background, objectives and relating research in the field.

- Chapter 2 includes an explanation of the conveyor system and the CST in detail. A closer look will be at the Hydraulic brake and the hydraulic actuator system surrounding it.

- Chapter 3 addresses modeling of the planetary gearbox and the kinematic model.

- Chapter 4 looks into the modeling of the clutch and the thermal generation and behavior.

- Chapter 5 explains the implementation done in simulink.

- Chapter 6 is dedicated to the sensitivity analysis of some of the components in the model.

- Chapter 7 compares some implementations and results for the model and components together with other models and site measurements data.

- Chapter 8 contains conclusions and reflections for the thesis and the earlier chapters. It also includes the possibilities for future work and improvements.

2

CST Description

Controlled Start Transmission is a gearbox design with integrated clutch pack. The main advantage with this type of transmission is the ability to control the transferred torque from the input to the output without a clutch in the torque transfer line which results in high efficiency at full speed.

2.1 Overview

The reducer transmission can be explained as one single planetary gear set combined with a wet clutch. The position of the clutch differs from a normal torque transfer clutch as that the wanted torque is not directly connected to the clutch but through a planetary gear set. The clutch connects the ring gear and the casing of the CST, acting as a brake for the ring gear. This is a common design in automatic transmissions, but then used for short high energy engagements. An example of an implementation of a CST can be seen in Figure 2.1.

There are no sensors for the speed of the ring gear but it can be estimated by measuring the output speed.

The system can be separated into two parts where one is the mechanical-hydraulic for the input-output torque transfer of the CST, and the other is a hydraulic control system for clutch actuation. The main cooling oil system is driven by a stand alone pump and cooled by a fan as seen in Figure 2.1. The oil is the same for the actuation of the clutch as the cooling and lubrication of the gearbox and all oil passes through the clutch for cooling as a part of the circulation. The actuation pump is driven by the main electric motor.
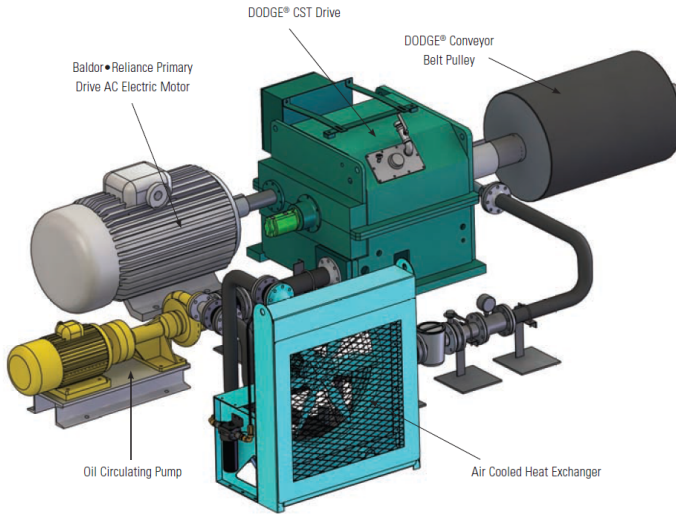
Figure 2.1: *Sketch of a CST system implementation, ABB/Baldor-Dodge*

2.2 Planetary Gear Set

A planetary gear set consists of three different gears shown in Figure 2.3, sun gear, ring gear and planet gear together with a planet carrier. The sun gear is identified as the blue gear, ring gear as the brown outer and the planet carrier as the green gear. The gear ratios are dependent on the relation between each gears rotational speed. The most common way to use a planetary gear set is to keep one gear stationary as the other are still free to rotate. The gear set inside the CST is presented in Figure 2.2 and be described as a reducer gearbox which increases the transferred torque. The sun gear is connected as the input gear and the carrier as the output. The ring gear controls the output speed by braking. When no torque is applied to brake the ring gear, the carrier is stationary as it often has more mass and larger inertia, which results in an increase of the ring gear speed until equilibrium is achieved. The reaction forces from the carrier load, the input motor torque and drag torque in the clutch decides when the equilibrium is met. The speed for the ring gear is proportional to the input motor speed.
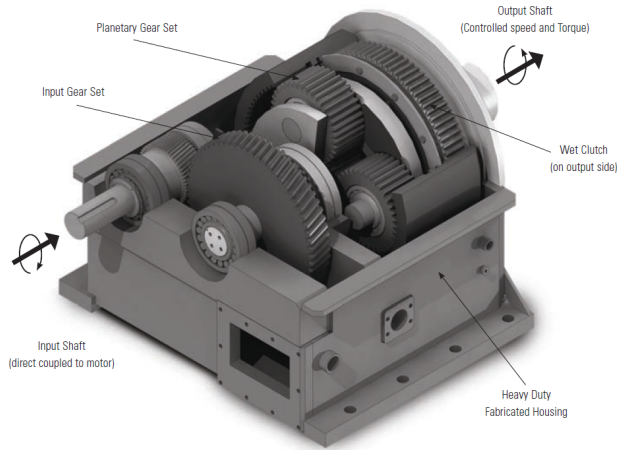
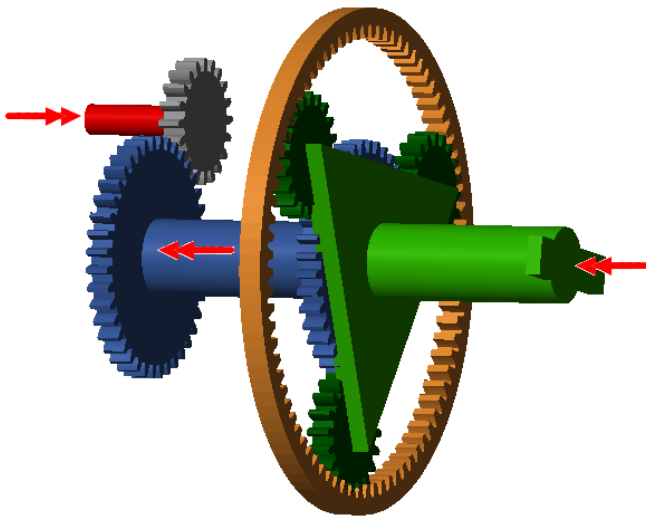*Figure 2.2:* *Closer look at the CST gearbox, ABB/Baldor-Dodge*

Figure 2.3: *Schematic view of a planetary gear set, red arrows marks rotation for normal operation.*

During an engagement, the pressure in the wet clutch increases which creates torque that acts on the ring gear as a brake. This forces the ring gear to slow down but gives a reaction on both the carrier and the sun/input gears. The electric motor that drives the input is set to keep a constant speed and increases the inserted torque to achieve this. The increased torque splits up between the ring gear and the carrier. When the speed of the ring gear decreases and the input speed is kept constant, the carrier is forced to increase its speed. This is a wanted

effect for this specific gearbox. The clutch brakes the ring gear until it is stationary and the carrier has achieved full speed. The whole engagement period is dependent on the load and the amount of mass that is connected to the carrier and needs to be accelerated.

2.3   Wet clutch

A wet clutch consists of several separator discs with alternatively friction discs. One side is mounted on the ring gear of the CST planetary gearbox and the other on the gear case. A circular piston is compressing the discs against each other and friction between the discs creates a braking torque. During the compression, oil passes through and cools the clutch. The whole clutch can be assumed to be submerged in oil. A sketch of a clutch is presented in Figure 2.4. The separator discs are usually made of steel and there are several different kinds of material and patterns for the friction discs. Common friction materials includes paper and sintered metal.
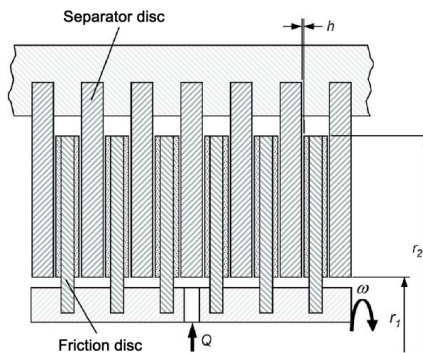

Figure 2.4: *Multi disc clutch, Yuan et al. [2007]*

During engagement the wet clutch behaves a little different from a regular dry clutch. As there is constant oil flow between the discs the oil needs to be squeezed out before contact is being made. This can be classified into three states of the clutch:

- Full film lubrication: The surfaces of the separator discs and the friction discs are completely separated by a fluid film.

- Mixed lubrication: The clutch compresses and the fluid film is shrinking which generates some hydrodynamic pressure which can influence the transfered torque.

- Boundary lubrication: The distance between the discs is very small and the discs are only separated by a thin layer of oil.

These different regimes go from a fully separated disc with full film lubrication

to boundary lubrication when the clutch is almost fully compressed. A limited slip differential (LSD) operates most of the time in the boundary lubrication state.

2.4   Hydraulic Actuation System

A hydraulic pump is driven by the CST sun axle and then powers up the system to a pressure of 1000 psi (69 Bar). This goes to a mounted block with Relief Valves (RV) which brings the system to a control pressure which is a little lower than the 69 Bar that the pump delivers. From here a PCV (Pressure Controlled Valve) is controlled by a PWM signal (Pulse Width Modulated signal) and that gives a pressure to the piston which compresses the clutch pack. A simple hydraulic schematic over the system is presented in Figure 2.5. The whole engagement is being controlled by a PLC which can monitor the CST and also an overall controller for the cite which can share a heavy load between several CST gearboxes.
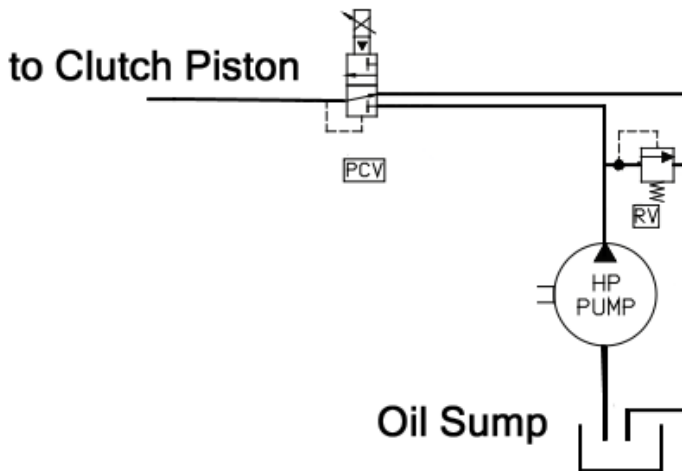

Figure 2.5: Simplified schematic over the hydraulic system

2.5   Cooling and Lubrication

To remove the heat generated by the clutch and to lubricate the planetary gear an external system has been implemented. A separate electric motor drives a hydraulic pump that pumps oil from the gearbox sump, through a cooling fan to have controlled temperature and then through the clutch. The oil flows through the clutch from the inside and out and denoted Q in Figure 2.4. The working pressure for the cooling/lubrication system is up to 100 psi (6.9 Bar), compared to the actuator pressure of 69 Bar. The external system makes it possible to have

the cooling system activated without having to activate the main motor. This is a advantage from a safety perspective and protection of the CST system.

3

Planetary Gear Modeling

The planetary gearbox is a more complex gear set than a regular set of gears but the dynamics can still be calculated using torque equilibrium equations. Calculating the correct speed of gear set components is important for the generated power.

3.1 Model Structure

In order to derive the dynamics of the gearbox, Torque equilibrium and the method described by Bai et al. [2013] is used. A sketch over the gearbox with torques and internal forces are presented in Figure 3.2. A kinetic constraint for the gearbox is applied to the velocities as

$$\omega_C(1 + \alpha) = \omega_S \alpha + \omega_R \tag{3.1}$$

$$\omega_S = -\frac{N_1}{N_2} \omega_{in} \tag{3.2}$$

$$\alpha = \frac{\omega_S}{\omega_R} = \frac{N_S}{N_R} = \frac{r_S}{r_R} \qquad \begin{aligned} N_i &= \text{Number of teeth on gear i.} \\ r_i &= \text{The radius of gear i.} \end{aligned} \tag{3.3}$$

N_1 and N_2 are the number of teeth on the input side of the gearbox and α is the gear ratio between the sun gear and the ring gear. In this case, a single planetary gear set is considered, so the ratio can be written as Equation (3.3)
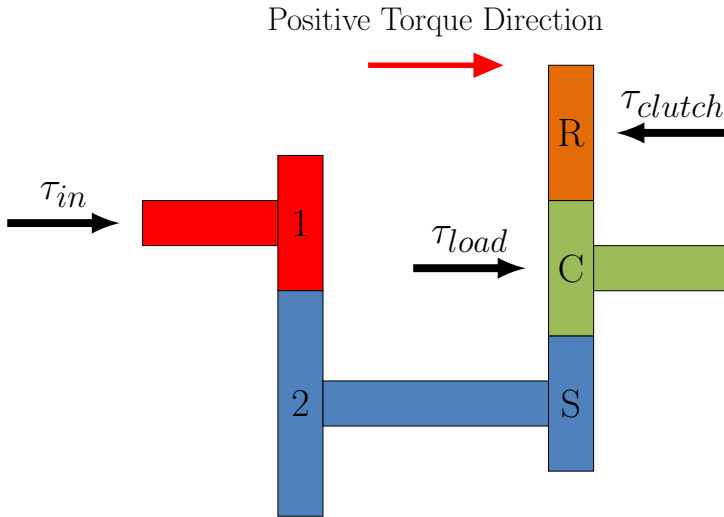
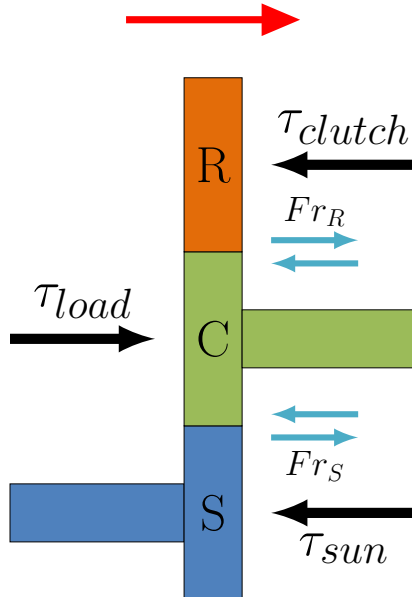**Figure 3.1:** *Schematic view over CST rotating bodies*

Figure 3.2: *Closer look at the planetary gear with internal torques*

The constraint is applied to the initial conditions in the model. The kinetic equations for the planetary gear set are written as three rotating bodies, each with the expression:

$$J_i \dot{\omega}_i = \sum \tau_{ext} \tag{3.4}$$

The rotating bodies is defined in Figure 3.1. Applying equation (3.4) to the rotating bodies presented in Figure 3.2 and results in the following equations for the gearbox:

$$\tau_{sun} = \frac{r_2}{r_1} \tau_{in} \tag{3.5}$$

$$J_S \dot{\omega}_S - F r_S = -\tau_{sun} \tag{3.6}$$

$$J_C \dot{\omega}_C + F(r_R + r_S) = \tau_{load} \tag{3.7}$$

$$J_R \dot{\omega}_R - F r_R = -\tau_{clutch} \tag{3.8}$$

The signs on τ_{sun}, τ_{load} and τ_{clutch} are made with rotational direction in mind. τ_{sun} drives the gears and the rotation direction of the sun is negative during normal operation. τ_{load} and τ_{clutch} acts on the system as "brakes" and the signs are opposite of the rotational direction during normal operation, which is positive sign for the ring gear and negative sign for the carrier. The inertias (J_i) are available for this thesis though it can be calculated as in Roos and Spiegelberg [2005]. To calculate the resulting model, Equations (3.5) to (3.7) are rewritten in matrix form as:

$$\begin{bmatrix} J & K \\ K^T & 0 \end{bmatrix} \Omega = \begin{bmatrix} \kappa \\ 0 \end{bmatrix} \tau \tag{3.9}$$

where:

$$J = \text{diag}(J_S, J_C, J_R) \tag{3.10}$$

$$\Omega = [\dot{\omega}_S, \dot{\omega}_C, \dot{\omega}_R, F]^T \tag{3.11}$$

$$K = \begin{bmatrix} -r_S \\ r_S + r_R \\ -r_R \end{bmatrix} \tag{3.12}$$

$$\kappa = \begin{bmatrix} -1 & 0 & 0 \\ 0 & 1 & 0 \\ 0 & 0 & -1 \end{bmatrix} \tag{3.13}$$

$$\tau = \begin{bmatrix} \tau_{sun} \\ \tau_{load} \\ \tau_{clutch} \end{bmatrix} \tag{3.14}$$

The dynamics of the four separate bodies are given through the inverse as:

$$\Omega = \begin{bmatrix} J & K \\ K^T & 0 \end{bmatrix}^{-1} \begin{bmatrix} \kappa \\ 0 \end{bmatrix} \tau \tag{3.15}$$

Then the model is divided into two parts: One for the dynamics for the gears and then one for the internal forces. The reacting forces are used to model the internal torque.

$$\begin{bmatrix} \dot{\omega}_S \\ \dot{\omega}_C \\ \dot{\omega}_R \\ F \end{bmatrix} = C \cdot \begin{bmatrix} M_{11} & M_{12} & M_{13} \\ M_{21} & M_{22} & M_{23} \\ M_{31} & M_{32} & M_{33} \\ M_{41} & M_{42} & M_{43} \end{bmatrix} \begin{bmatrix} \tau_{sun} \\ \tau_{load} \\ \tau_{clutch} \end{bmatrix} \tag{3.16}$$

The internal force is the last row of Ω. The values of $M_{i,j}$ are presented in Appendix A.1 as they are large and space consuming.

3.1.1   Simplifications

In this kinetic model some simplifications are made:

- No friction from the bearings are accounted for.
- Torque from the hydraulic pump acting on the sun axle is neglected.
- No mechanical efficiency is included. These simplifications are made to keep the complexity of the model down.

3.2   Planetary Gear Validation

For the dynamics, a reference ramp is simulated with a PI-regulator controlling the speed of the ring gear via τ_{clutch} input signal such that $\omega_R = \omega_{ref}$. This is to simulate the ramping up of the output carrier speed. The carrier starts at stand still. The ramp starts at t=15 s and the ring gear is to be at a complete standstill 25 s later. The input is kept constant using the reaction force F and Equation (3.6). The acceleration is set to zero ($\dot{\omega}_s = 0$) by the input torque:

$$\tau_{sun} = Fr_1 \tag{3.17}$$

The reason for doing this is to simulate an electric motor that can deliver all torque needed to keep a constant velocity. The load torque (τ_{load}) is constant and set to 400 Nm. Figure 3.3 shows that the system has a good following and the PI-regulator can control how much torque is needed to control the ring gear.
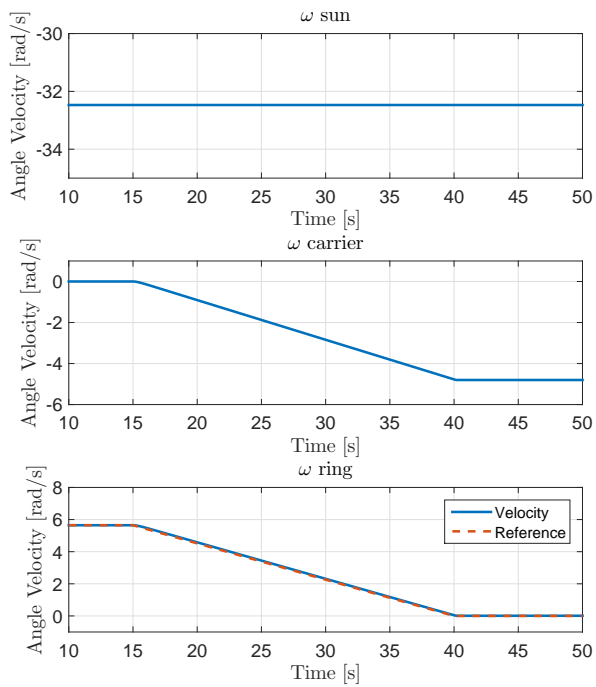
Figure 3.3: *Simulated planetary transmission: Reference for ω_{Ring} starts at time 15 s, transmission velocities.*
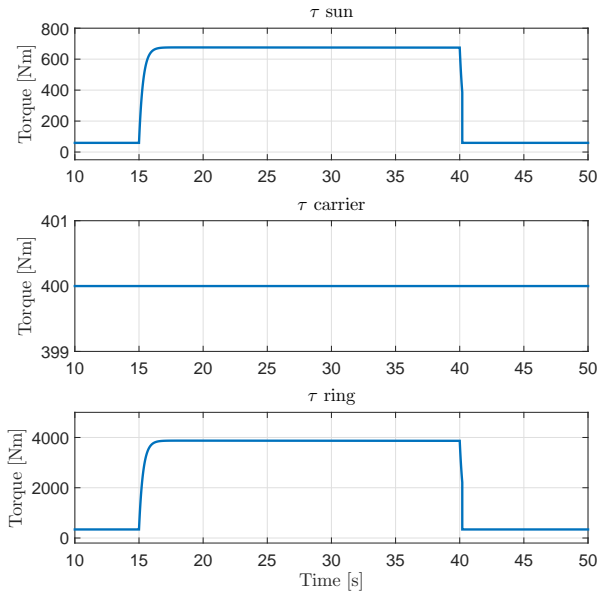
Figure 3.4: *Simulated planetary transmission: Reference for ω_{Ring} starts at time 15 s, torques on the gears.*

The behavior seems proper as the ring gear brakes to a stop and the carrier speeds up to its target speed according to Figure 3.3. In Figure 3.4 one can see that the torque acting on the gears is proper and the size is a result of a large inertia on the output gear. Both the ring gear and the input gear have increasing torque which is expected to keep a constant load on the carrier as the ring gear speed (ω_R) is decreasing. In the time t < 15 s and t > 40 s the torque on the input and the clutch is directly related to the constant load according to Equation (3.6) to (3.8) and ($\dot{\omega} = 0$) as

$$\tau_{sun} = \frac{1}{(1 + \frac{r_R}{r_S})} \tau_{carrier} \tag{3.18}$$

$$\tau_{ring} = \frac{1}{(1 + \frac{r_S}{r_R})} \tau_{carrier} \tag{3.19}$$

4

Clutch Torque and Temperature Modeling

The models for the clutch and the temperature distribution are presented in this chapter.

4.1 Clutch Model

In this chapter a model for the clutch is assembled and tested for a proper behavior. The model is based on the clutch model of Bai et al. [2013], friction model from Deur et al. [2005] and Ivanović et al. [2009] with a modification. The models are from LSD applications and differs from wet clutch engagement models, since the oil compression torque in the clutch is neglected. This is due to an observation of the slow system transients and further explained in Section 4.1.1.

4.1.1 Hydrodynamics

The engagement of a hydraulic clutch can be divided into three parts: hydrodynamic lubrication phase, partial lubrication phase and mechanical contact phase. The last one can also be called boundary friction phase. The hydrodynamic phase and the partial lubrication phase are the first phases when the clutch is engaged and the fluid between the discs in the clutch is compressed which increase the transferred torque. The influence on the transferred torque is dependent on the squeeze speed which the discs are compressed with and often described with a Reynolds equation for the disc distance h and the squeeze speed $\frac{dh}{dt}$. The Reynolds equation is a common way to model fluid film dynamics but is complex and demanding to parametrize (Ivanović et al. [2011]). As the oil film is shrinking, so does the influence on the transferred torque. The impact on the torque from the thin film dynamics are negligible after a short while, depending on the engagements speed. Using the result from Marklund and Larsson [2007]

and Jin et al. [2014], the torque are simulated and it is found that the hydrody-
namic torque is small at the end of the engagement and negligible after a period
of time. This period of time varies for different systems. In this thesis the hydro-
dynamic influences including the partial lubrication phase are neglected as the
engagements speed is assumed slow and in continuous slip for the whole engage-
ment.

4.1.2   Model Structure

The transferred torque is mostly similarly looking throughout the literature. Of-
ten modeled as a linear function of pressure acting on the clutch as

$$\tau_{trans} = \mu \cdot N_f \cdot R_e \cdot F_{app}(p) \tag{4.1}$$

$$F_{app} = A_{pist} \cdot p - F_{spring} \tag{4.2}$$

Here τ_{trans}, N_f, R_e, A_{pist} represent transferred torque, number of frictions sur-
faces, effective radius of the clutch and the clutch piston area. The model for the
friction coefficient μ is expanded with a dependency on temperature as:

$$\mu = \mu(T) = C_1 T + C_2 \tag{4.3}$$

This friction model is easier to parametrize from data than the more complex fric-
tion models according to Ivanović et al. [2009]. To identify the friction parame-
ters one can do a pin-on-disc investigation as described in Marklund and Larsson
[2008]. This is a cheaper and simpler way to identify friction parameters than the
standard full clutch experiment. The return spring force is proportional to the
piston position but fitted to measurement data as a constant described in section
4.1.1. The transferred torque is using a hyperbolic tangent function to handle
characteristics as the slip speed approaches zero. The slip speed is defined as $\Delta\omega$
$= \omega_{slip}$. In reality when $\omega_{slip} = 0$, the maximum torque is transferred, except in
these kind of applications. The clutch acts like a brake and cannot accelerate the
gear in opposite direction past standstill. The final torque model structure based
on Equation (4.1) becomes:

$$\tau_{clutch} = \mu(T) \cdot F_{app}(p) \cdot R_e \cdot N_f \cdot tanh(\omega_{slip}/\gamma) + \tau_{visc,fric}(\omega_{slip}) \tag{4.4}$$

$$R_e = 2/3 \frac{R_{outer}^3 - R_{inner}^3}{R_{outer}^2 - R_{inner}^2} \tag{4.5}$$

$$F_{app} = A_{piston} \cdot p - F_{spring} \tag{4.6}$$

$$\tau_{visc,fric} = \beta_v |\omega_{slip}| = \frac{N_f \mu_{dyn} \pi \left(R_2^2 - R_1^2\right) r_m^2}{h_{max}} |\omega_{slip}| \tag{4.7}$$

During motor startup, when the clutch is disengaged, there is oil flowing through
the clutch as the speed of the clutch starts to build. When the motor is at work-

ing speed the clutch is at peak speed as well. The presence of oil between the discs generates a viscous braking torque based on sheering of the oil depending on the slip speed ω_{slip} and properties on the oil. That drag friction is lumped together to make a drag torque that is acting on the clutch as Equation (4.7) based on the result from Kitabayashi et al. [2003]. This gives an approximate of the drag torque generated when the clutch is disengaged and the distance h is kept constant. Here μ_{dyn}, h_{max} and r_m represent the dynamic viscosity of the oil, the maximum distance between the friction discs and separator disc and the mean disc radius. The dynamic viscosity μ_{dyn} is calculated as:

$$\mu_{dyn} = \nu\rho_{oil} \qquad \begin{aligned}&\nu = \text{Kinematic viscosity}\\&\rho_{oil} = \text{Density of the oil}\end{aligned} \qquad (4.8)$$

Where the kinematic viscosity and density are common parameters found in data sheets. γ is a scale parameter to control how the torque behaves when the speed approaches zero.

4.2   Thermal Model

The temperature model is based on Ivanović et al. [2009] and the temperature of a single separator disc is modeled. The reason for modeling a single disc instead of the whole clutch pack is that it is hard to measure temperature in a large mass, and in an experimental environment a thermo couple would be placed in a single separator disc only. The temperature generation is dependent on the surface speed and this gives a temperature that is dependent on the radius. In order to keep the complexity of the model down, a mean value model is used for the whole disc. The difference of temperature across the disc is not large according to CFD simulations by Abdullah and Schlattmann [2014] and investigations by Marklund et al. [2007] found that the temperature is highest around the effective radius.

A constant temperature of the cooling medium is assumed. In reality, the oil heats up and gives a less effective removal of generated heat. The amount of available oil and the cooling system makes the assumption reasonable. The ambient temperature is the same as the oil temperature. This approximation implies that the casing also has the same temperature and does not heat up during the engagement.

4.2.1   Model Structure

The model is based on power balance and heat generated when the clutch is braking. This model uses a lumped parameter, dominated by convectional heat transfer as the conductive heat transfer is small enough to neglect. This is a common simplification done often in the literature (Deur et al. [2005], Marklund and Lars-

son [2007]). The generated heat (P_{gen}) is modeled as:

$$P_{gen} = \frac{\omega_{slip}\tau_{clutch}}{N_{sep,discs}} \qquad [W] \tag{4.9}$$

The generated heat divides on all the discs in the clutch. The heat transferred, removed from clutch, depends on the medium used for cooling. The Heat Transfer Coefficient (HTC) is a function of many parameters that can be difficult to calculate analytically so the approach is to identify this function through experiment. This gives a lumped HTC that also considers conductive heat transfer and other losses including heating of the case and the friction discs. The amount of heat removed from the clutch disc is described as

$$P_{removed} = HTC(\cdots) \cdot A_{clutch} \cdot (T_{SD}(t) - T_{amb}) \qquad [W] \tag{4.10}$$

T_{amb} is the temperature of the cooling medium, in this case a combination of lubricant and hydraulic oil, A_{clutch} is the clutch area and T_{SD} the temperature of the modeled separator disc. The resulting surplus of power generated is then distributed throughout the separator disc. The resulting HTC function from Ivanović et al. [2009] is applied as an interpolated lookup table together with a delay and first order dynamics with separate time constants for a rising and falling HTC and are experimentally identified. The HTC-function becomes:

$$HTC = HTC_{table}(F_{app}(p), \omega_{slip}) \cdot G(s) \tag{4.11}$$

$$G(s) = \frac{e^{-\tau_{delay}s}}{\tau_i s + 1}, \qquad \begin{array}{l} \tau_i = \text{Rising "1" or falling "2" flank time constant} \\ \tau_{delay} = \text{Delay time for the HTC parameter} \end{array} \tag{4.12}$$

The resulting look up table is shown in Figure 4.1 and the data used for this table are presented in Figure 14 in Ivanović et al. [2009]. The applied force is limited to 18 kN which is low for a CST application and thus the removal of heat in Equation (4.10) is fitted to a clutch with both smaller radii and fewer discs.
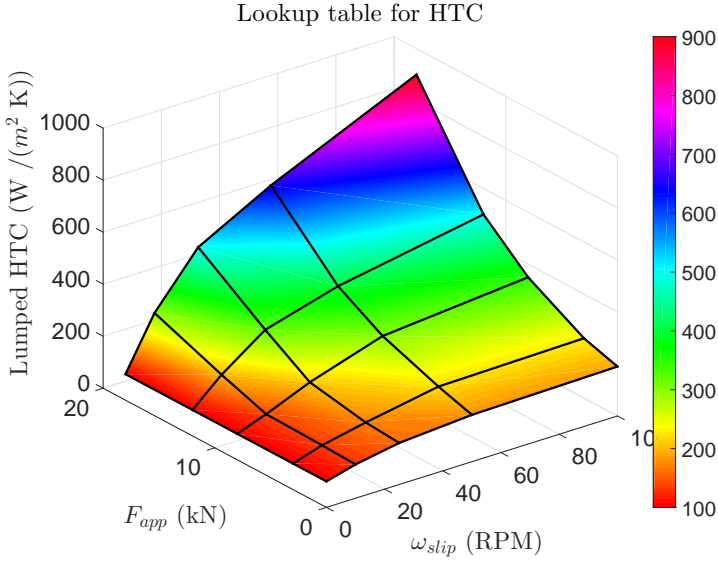
Figure 4.1: *Surface plot of interpolated HTC lookup table.*

The temperature dynamics of the separator disc is described as:

$$\dot{T}_{SD}(t) = \frac{1}{\rho_{SD} V_{SD} C_{p,SD}} [P_{gen} - P_{removed}] = \frac{1}{M_{SD} C_{p,SD}} [P_{gen} - P_{removed}] \qquad (4.13)$$

ρ_{SD}, V_{SD} and $C_{p,SD}$ represents the density, volume and specific heat capacity of the clutch separator disc. ρ_{SD} and V_{SD} can be combined to the mass of the disc:

$$M_{SD} = \rho_{SD} V_{SD} \qquad (4.14)$$

4.3 Model Validation

Validation of the models is done by using comparison with the literature. In order to validate the clutch and temperature models some estimations are needed.

4.3.1 Separator Disc Temperature Model (T_{SD})

From Ivanović et al. [2009] the effective radius r_e is given. Using this, Equation (4.5) and nonlinear curve fitting one can extract <u>one</u> proper inner and outer radii as Equation (4.15) to (4.17). This approach is very dependent on the starting

points of the curve fitting.

$$R_e = 0.049 \ m \qquad \text{(Ivanović et al. [2009])} \qquad \Rightarrow \qquad (4.15)$$

$$R_{outer} = 0.0628 \ m \qquad\qquad\qquad\qquad\qquad\qquad (4.16)$$

$$R_{inner} = 0.0318 \ m \qquad\qquad\qquad\qquad\qquad\qquad (4.17)$$

This is done with the initial values of 6 cm and 3 cm for outer and inner radius. It is assured that this is not the only combination of radii but it is the one used for this validation. Using these radii to calculate the area and then estimating the thickness (d_{SD}) to get some proper response from the model in (4.13). The area and thickness are estimated as:

$$A_{clutch} = \pi \left(R_{outer}^2 - R_{inner}^2 \right) = 0.0092 \ m^2 = 92 \ cm^2 \qquad (4.18)$$

$$d_{SD} = 2 \ mm \qquad\qquad\qquad\qquad\qquad\qquad (4.19)$$

$$V_{SD} = A_{clutch} \cdot d_{SD} = 1.8463 \cdot 10^{-5} \ m^3 = 18.46 \ cm^3 \qquad (4.20)$$

Using these parameters one can now compare the plots to the results in Ivanović et al. [2009]. Evaluating the separator disc temperature behavior from a step in rotational speed (ω_{slip}), the simulated response can be seen in Figure 4.2 and a good fit can be seen compared to Figure 17 in Ivanović et al. [2009]. The temperature is a bit lower but it can be explained by the errors in estimated areas and volumes. All the parameters are according to Table 4.1 and the step is from 25 rpm to 10 rpm according to Figure 17 in Ivanović et al. [2009].

| Symbol	Parameter	Value
τ_{clutch}	Clutch torque	130 Nm
$N_{sep,discs}$	Number of separator discs	2
A_{clutch}	Area of the clutch surface	92 cm^2 (4.18)
V_{SD}	Volume of separator disc	18.46 cm^3
ρ_{SD}	Density of separator disc (Steel)	7850 kg/m^3
$C_{p,SD}$	Specific heat capacity of separator disc (Steel)	450 J/kgK
T_{amb}	The ambient temperature	32 ° C
τ_1	Time constant for rising HTC parameter	1 s
τ_2	Time constant for falling HTC parameter	2.5 s
τ_{delay}	Time delay for HTC parameter	2 s

Table 4.1: *Parameters used for validation*
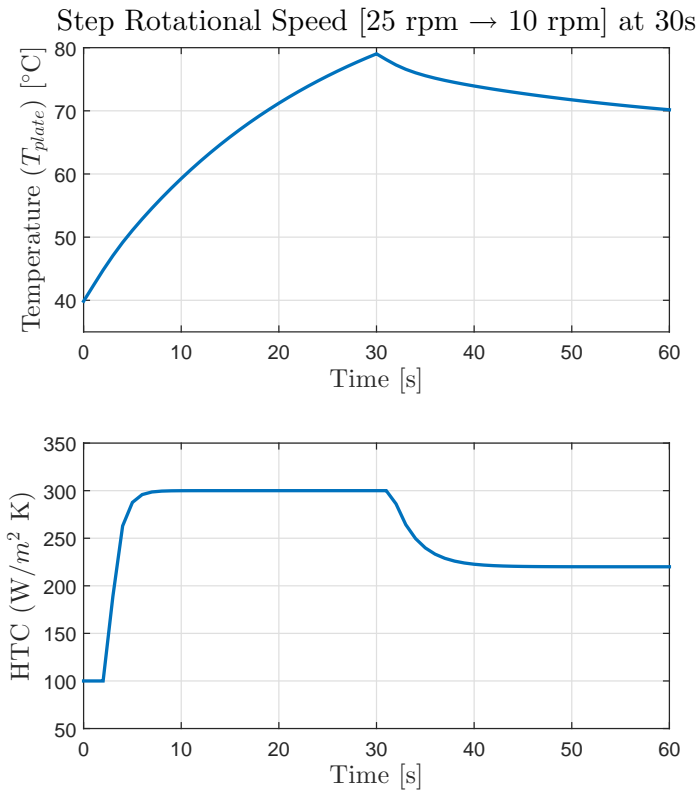
Figure 4.2: *Simulated step response. The temperature is shown in the upper figure and the HTC in the lower.*

The temperature behavior is similar to the paper and the difference can be the insecurities from the area and volume estimations. The HTC function has a good fit which is expected as it is directly imported from the paper.

4.3.2   Clutch Torque Model

Looking at the clutch torque transfer in Equation (4.4) and also in Figure 17 in Ivanović et al. [2009], it is clear that F_{app} and τ_{clutch} are closely correlated. Using the temperature result from the previous validation the clutch torque model can be validated by keeping a constant F_{app} and looking at the transferred torque. The parameters in this validation are similar to Table 4.1 and the changes are presented in Table 4.2. The friction parameters C_1 and C_2 from equation (4.3) are estimated from Figure 9 in Ivanović et al. [2009]. A mean value is estimated for the highest F_{app} and a slip speed of 50 rpm. The result can be seen in Figure 4.3.

Symbol	Parameter	Value
F_{app}	Applied force acting on the clutch	12 kN
τ_{clutch}	Clutch torque	Modeled
N_f	Number of friction surfaces	2
β_v	Viscous drag torque parameter	0
C_1	Friction parameter 1	$-1.35 \cdot 10^{-4}$ $1/°C$
C_2	Friction parameter 2	0.12

Table 4.2: Parameters used for validation
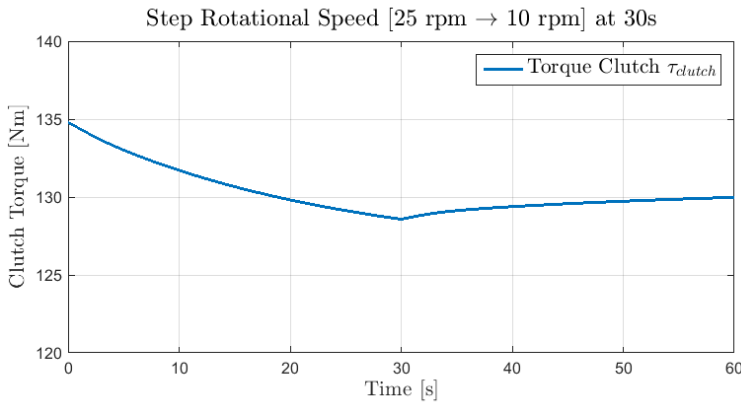
Figure 4.3: Validation: Simulated step response of torque. This compares to the measured clutch torque shown as the blue dashed signal in the upper part of figure 17 in Ivanović et al. [2009].

When comparing the torque in Figure 4.3 and the lower plot in figure 17 in

Ivanović et al. [2009], one can see the stationary torque have an acceptable fit. The measured torque can be seen as the dashed blue line in the lower part of the upper plot. It shows a torque around 130 Nm and similar values can be seen by the simulated torque model below. The simulation does not seem stable during the step and this is because the torque is modeled with a dependency on the temperature.

5

Implementation

Here the implementations in MATLAB and Simulink are presented and explained. An overview of the model is presented in Figure 5.1 and the scopes and available measurements are presented in Figure 5.2.
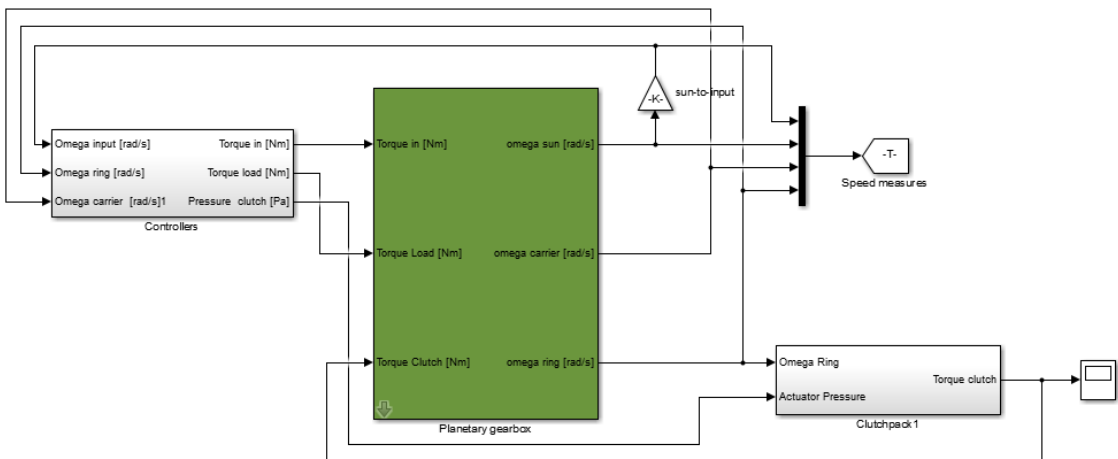
Figure 5.1: *Overview of the Simulink model*
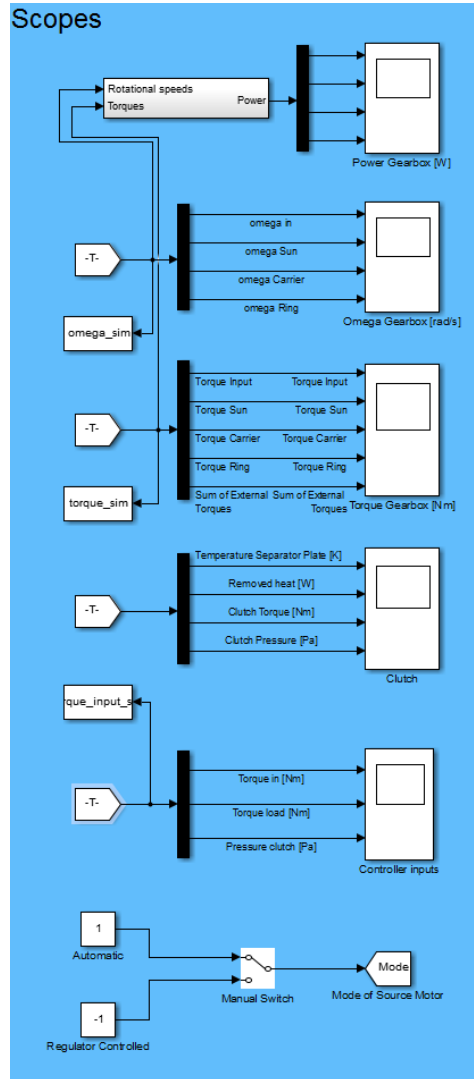
Figure 5.2: *The available scopes for the model*

The controller block contains a PI-controllers for the ring speed (ω_R) and input gear speed (ω_1). The control outputs are input torque (τ_{in}) and clutch pressure (p). The tuning of PI-parameters is not of any importance.
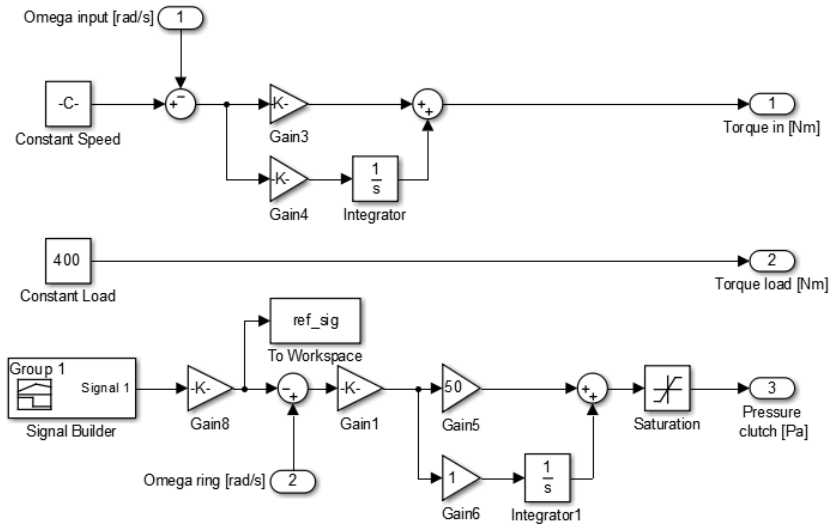
Figure 5.3: Contents of the controller block

5.1 Planetary Gearbox

The gearbox is implemented as a masked block with three inputs ($\tau_{in}, \tau_{load}, \tau_{clutch}$) and four outputs ($\dot{\omega}_S, \dot{\omega}_C, \dot{\omega}_R, F$). The dynamics of the planetary gearbox are implemented as a MATLAB function as can be seen in Figure 5.4.
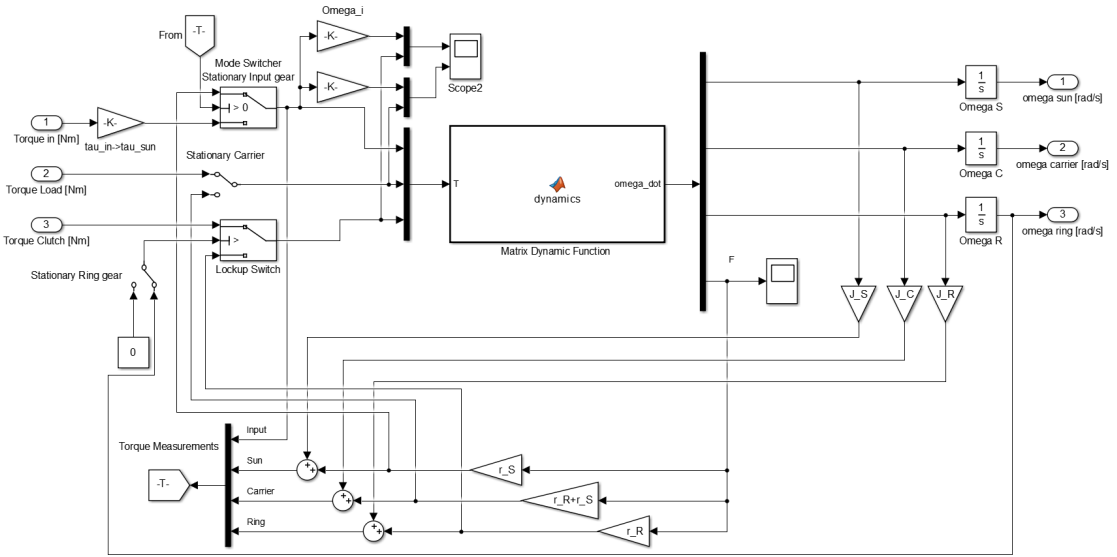
Figure 5.4: *Planetary gearbox implemented in Simulink.*

The function is an implementation of Equation (3.15).

$$\Omega = \begin{bmatrix} J & K \\ K^T & 0 \end{bmatrix}^{-1} \begin{bmatrix} \kappa \\ 0 \end{bmatrix} \tau \qquad\qquad \text{(3.15 revisited)}$$

The different accelerations ($\dot{\omega}_i$) are then integrated to accumulate the rotation speeds (ω_i). To handle the clutch lockup, a switch function according to the slip speed is used. When the speed of the ring becomes lower than a given tolerance, the torque input is changed to keep the acceleration to zero as

$$\tau_{clutch,in} = \begin{cases} \tau_{clutch} & \omega_R > \omega_{R,tol} \\ -Fr_R & \omega_R \leq \omega_{R,tol} \end{cases} \qquad\qquad (5.1)$$

Note that $-Fr_R$ is equal to τ_{clutch} in Equation (3.8) if the acceleration $\dot{\omega}_R =0$. Equations (5.1) and (4.1) are used to calculate a required pressure to keep the clutch stationary. In the bottom left corner in figure 5.4, the torques are calculated according to equations (3.5) to (3.8) and sent to scopes. All the inputs of the parameters are made through the mask as figure 5.5 shows. The inputs are teeth number, inertias for all of the gears, start values for the carrier and input axle and the radius of the gears, apart from this a settings file exists for all of the parameters.

Figure 5.5: Planetary gearbox mask.

5.2   Clutch and Temperature

The clutch and temperature are implemented in the same block "Clutchpack" in Figure 5.1. The block is presented in Figure 5.6 and one can see the separation of the temperature model and torque transfer model.
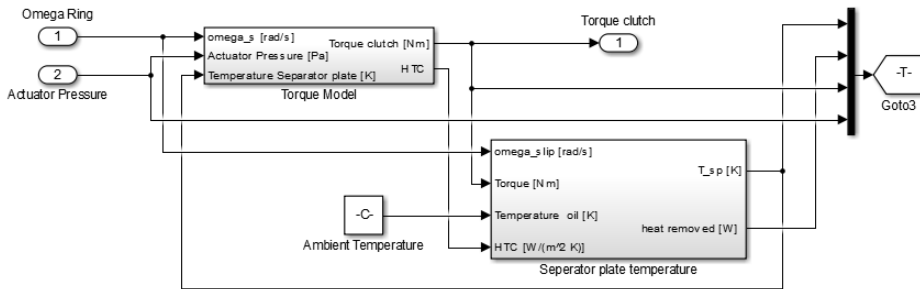

Figure 5.6: Clutchpack implemented in Simulink

The ambient temperature is assumed constant and the HTC is generated by a lookup table. The torque transfer model is implemented as in Figure 5.7. The friction block is implemented according to Equation (4.3) and the basic function is according to Section 4.1.2. The saturation is there to prevent a constant spring force to result in negative torque for low actuator pressures.
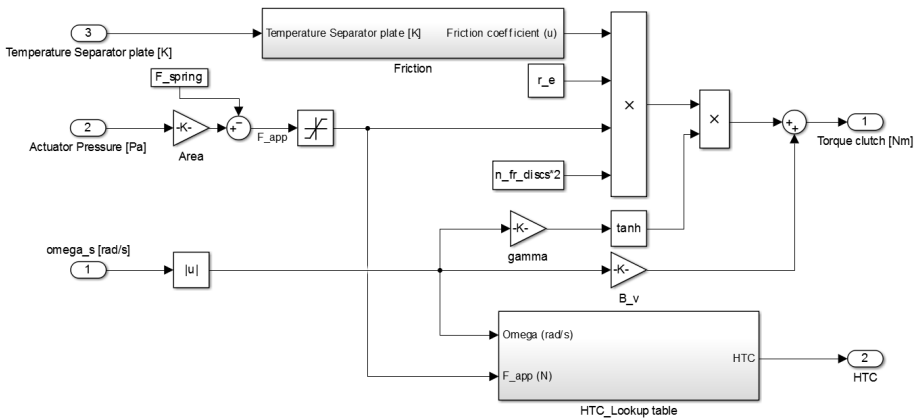
Figure 5.7: Clutch torque transfer implemented in Simulink

The lookup table for the HTC is also placed in the block where the clutch torque is generated and its implementation can be seen in Figure 5.8.
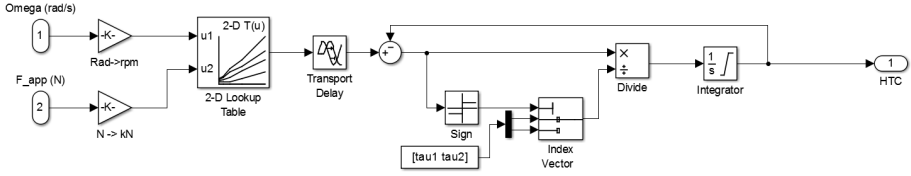
Figure 5.8: *HTC lookup table, implemented using the result in Ivanović et al. [2009]*

The model for the temperature is an implementation of Equation (4.13) and presented in Figure 5.9. The ambient temperature T_{amb} is set to $40°C$ and the initial temperature is also set to this temperature.
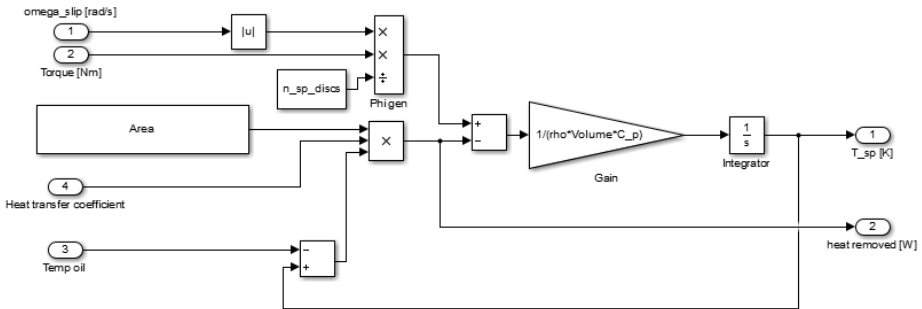

Figure 5.9: *Temperature model implemented in Simulink*

6

Sensitivity Analysis

To get an idea of how sensitive the temperature and clutch models are with respect to different model parameters, a sensitivity analysis is conducted. The analysis is concentrated on the clutch and thermal model and the parameters included in those models. The gearbox model is too heavily dependent on the controller and would not give a good comparison for the overall model.
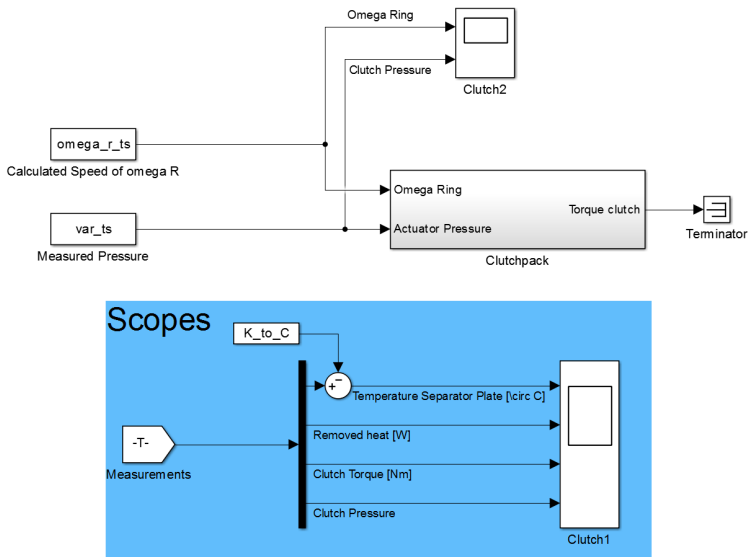

Figure 6.1: Simulink implementation of the sensitivity analysis.

6.1   Method

The analysis is performed with data from a commission of a conveyor site where a CST is used. The clutch pressure and speed of the load are measured and this is enough to get an idea of the temperature inside the clutch. The input speed is considered constant and known. The clutch slip speed (ω_s) can be estimated as a function of the output speed as Equation (6.1). The simulink implementation can be seen in Figure 6.1. A modification is made to the clutch model shown in Figure 6.2 and consists of a simple check if the system is inserting power. This modification is made due to the viscous torque is generating heat even if no power is inserted to the system. This is a direct result of the ring speed ω_R being directly proportional to the output speed ω_{load} and keeping ω_{in} constant.

$$\omega_R(\omega_C) = \omega_C(1 + \alpha) + \frac{N_1}{N_2}\alpha\omega_{in} \tag{6.1}$$

Figure 6.2: Modification of the clutch simulink model

The method used is a simple one-at-a-time (OAT) sensitivity analysis. This means that one parameter is disturbed/modified, simulated and compared to a reference simulation ($T_{ref}(t)$). This is repeated for all the parameters that are investigated. The levels investigated are ±10% and ±20% of the current parameters. The result is stored in a simulated temperature series ($T_{sim}(t)$). To compare the different parameters with each other, a comparison value is constructed from a normalized error as following.

$$R_2(t) = \left(\frac{T_{sim}(t) - T_{ref}(t)}{T_{ref}(t)}\right)^2 \tag{6.2}$$

$$R_{comp} = \sum_{t=0}^{t=max} R_2(t) \tag{6.3}$$

This gives an indication of how much a parameter impacts the whole engagement

with a single value. Some parameters are easier to estimate and have a physical meaning such as areas and volumes, but some need extensive investigations and estimations to have a good fitting. The measurements used in this analysis are from two consecutive engagements.

6.2   Results and Discussion

The result of the simulations and the comparison values are presented in Table 6.1. Notable is the large number for the ambient temperature. This is because of the stationary error that this parameter changes. When investigated further in Figure 6.3 one can see that the curves have a bias, which is expected as the reference temperature is modified. All of the sensitivity plots are presented in Appendix B and the parameters with the largest deviations are presented below.

Parameter	Modification			
	+20%	**+10%**	**-10%**	**-20%**
Piston Area	4.6417	1.2414	1.4896	6.1072
Friction coefficient 1	0.0121	0.0030	0.0031	0.0124
Friction coefficient 2	1.8153	0.4538	0.4538	1.8153
Separator disc volume	0.6419	0.1778	0.2208	0.9910
Clutch Area	1.8487	0.5494	0.8133	4.0755
Viscous Friction (β_v)	0.0732	0.0183	0.0183	0.0732
Clutch Parameter (γ)	0.0371	0.0107	0.0149	0.0715
Ambient Temperature	95.2032	23.8008	23.8008	95.2032
Return Spring Force	2.4184	0.6187	0.6714	2.8498

Table 6.1: *Summary of R_{comp}*

The maximum temperature presented in Table 6.2 gives a similar indication as the R_{comp} presented in Table 6.1.

Parameter	Modification			
	+20%	**+10%**	**-10%**	**-20%**
Piston Area	15.8193	8.3568	9.2166	18.6092
Friction coefficient 1	0.8513	0.4272	0.4302	0.8634
Friction coefficient 2	9.7322	4.8661	4.8661	9.7322
Separator disc volume	5.3685	2.8504	3.2464	6.9662
Clutch Area	5.8340	3.0731	3.4427	7.3293
Viscous Friction (β_v)	1.4562	0.7281	0.7281	1.4562
Clutch Parameter (γ)	0.2523	0.1356	0.1589	0.3465
Ambient Temperature	8.0000	4.0000	4.0000	8.0000
Return Spring Force	11.4464	5.8899	5.6291	10.9593

Table 6.2: *Maximum temperature difference (°C)*
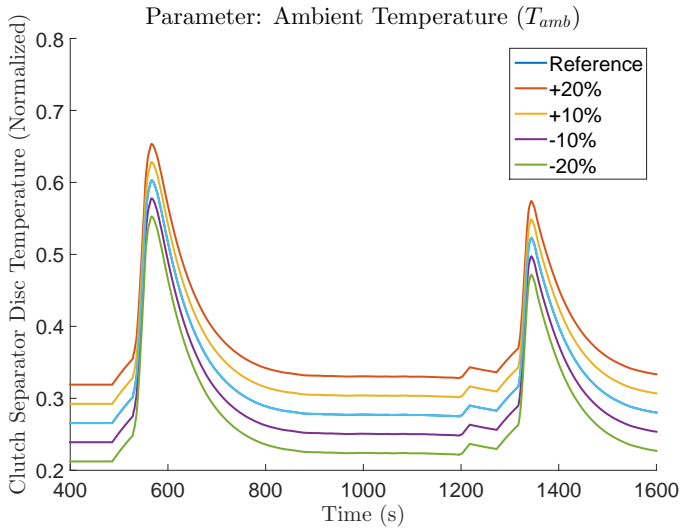
Figure 6.3: *Sensitivity analysis for the ambient temperature parameter.*

The four most sensitive parameters are marked in Table 6.1 and investigated further by looking at the transient behavior in the simulation. Before using the HTC lookup table the sensitivity of a constant value of HTC is investigated.
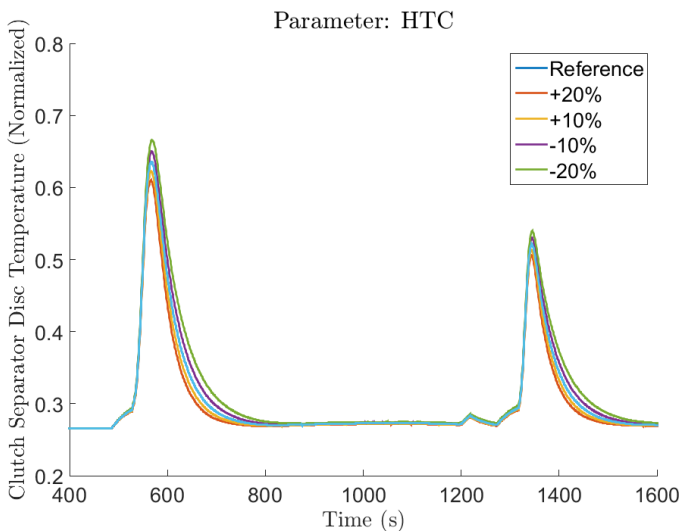
Figure 6.4: *Sensitivity analysis for a constant HTC (375 W/ m^2 K). This is an earlier model but included for reference.*

One can see from Figure 6.4 that the largest differences are the peaks and the cooling rate. The parameter controls how much of the heat generated is removed to heating the oil and housing. This parameter was replaced with a lookup table described in Section 4.2 but this shows how sensitive the parameter is with respect to errors in the lookup table as well.
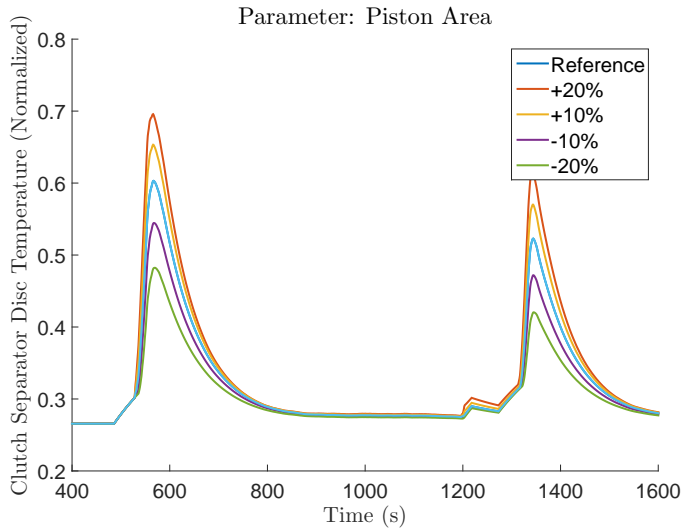
Figure 6.5: *Sensitivity analysis for the clutch piston area.*

The piston area is a sensitive parameter as it directly affects the applied force, and therefore the generated heat. A good thing is that the parameter is a physical value and can be measured easily. The same applies to the clutch area parameters in Figure 6.6. The area is a sensitive parameter as the amount of heat removed is directly affected by this parameter.
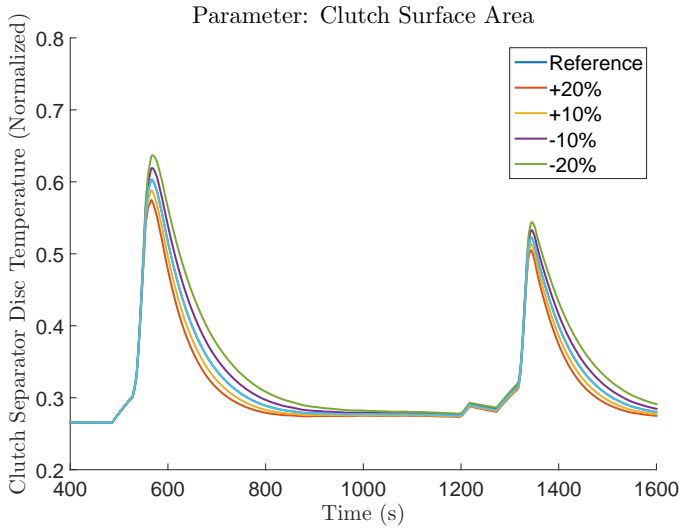
Figure 6.6: *Sensitivity analysis for the clutch surface area.*
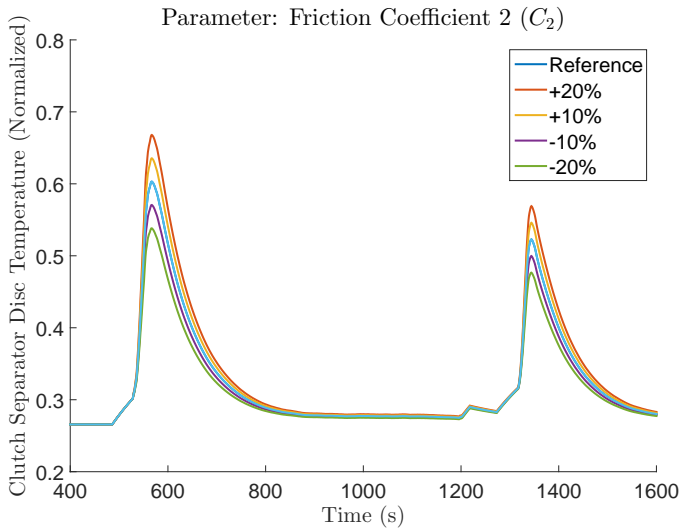
Figure 6.7: *Sensitivity analysis for friction coefficient 2.*

The friction coefficient has a big influence on the model and it is a difficult parameter to estimate. This is a field in itself and as shown in Figure 6.7 has a big impact on the result.

6.2.1 Summary

The Clutch and Temperature models are sensitive and different parameters impact the model more than others. There is also a difference between measurable parameters such as area and volume, and estimated parameters as the friction coefficients and the HTC. The focus should be according to the estimating parameters:

    1: Friction coefficients

    2: The return springs

    3: Correct areas for both the piston and clutch surface.

It is also important to have a correct ambient temperature model to get a good reference level for the overall model. The area is sensitive as well but it is not an estimated variable but a measurement. One thing to include is that the sensitivity analysis can also be applicated on the transferred torque. The parameters connected to the generated torque are the piston area, friction coefficients and the return spring force F_{spring}.

7

Results and Discussions

To get some idea of the model fit, investigations of temperature generation and possible energy saving possibilities are made using measurements from a commission of a conveyor system at Titania A/S, Norway. The measurements available were logged from the PLC and control system. The measurements are normalized with a nominal value making the values unit less. The clutch torque and power is in focus as no measurements of temperature are available from the site.

7.1 Method

The method used is the same as the sensitivity analysis but the focus is towards the power and clutch torque instead of the temperature. To get a good estimation of the temperature, one of the most important parts is to get the generated heat correct and as we can measure the rotational speed the estimated torque is investigated. To get an idea of the size of the torque inside the gearbox, the Equations (3.5) trough (3.8) are revisited:

$$\tau_{sun} = \frac{r_2}{r_1} \tau_{in}$$
$$J_S \dot{\omega}_S - F r_S = -\tau_{sun}$$
$$J_C \dot{\omega}_C + F (r_R + r_S) = \tau_{load}$$
$$J_R \dot{\omega}_R - F r_R = -\tau_{clutch}$$

Assuming the gearbox is at stationary operation and the acceleration is zero, one can get an estimation of the resulting torque by using the input torque ($\tau_{input,motor}$)

and Equation (7.2) and (7.3).

$$\overset{(3.6),(3.5)}{\Rightarrow} F = \frac{r_2}{r_1 r_S} \tau_{in} \tag{7.1}$$

$$F(r_R + r_S) = \tau_{load} \overset{(7.1)}{\Rightarrow} \tau_{load} = \underbrace{\frac{r_2}{r_1}(1 + \frac{r_R}{r_S})}_{=:\Theta_{load}} \tau_{in} = \Theta_{load} \tau_{in} \tag{7.2}$$

$$Fr_R = \tau_{clutch} \overset{(7.1)}{\Rightarrow} \tau_{clutch} = \underbrace{\frac{r_2 r_R}{r_1 r_S}}_{=:\Theta_{clutch}} \tau_{in} = \Theta_{clutch} \tau_{in} \tag{7.3}$$

Using Equation (6.1) from the sensitivity analysis the rotational speed is calculated with the input speed (ω_{input}) set constant:

$$\omega_R(\omega_C) = \omega_C(1 + \alpha) + \frac{N_1}{N_2} \alpha \omega_{in} \tag{6.1 revisited}$$

The implementation in simulink is shown in Figure 7.1 and the clutch block is the same as in Section 5.2 and the modification described in Section 6.1.
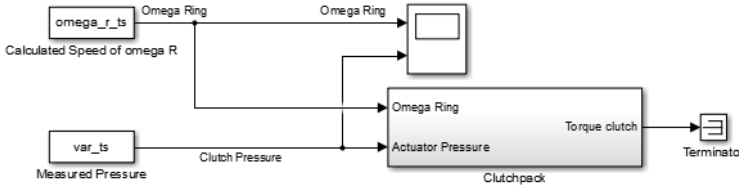
Figure 7.1: *Implementation in Simulink for simulations using measured input signals.*

7.1.1   Idle Bias Removal

During operation, power is used to drive the motor and overcome frictional losses. These are removed from the input power as these are not contributing to the torque transfer. The removal is done by

$$\tau_{in,0} = \frac{P_{in}}{\omega_{in}} \tag{7.4}$$

$$\tau_{in} = \tau_{in,0} - (\tau_{comp} - \tau_{visc,max}) \tag{7.5}$$

Where τ_{comp} represent the compensated torque, the amount of torque needed to turn the CST without moving the load. It is presented in Figure 7.2 and included is the viscous torque that clutch generates during idle drive. Represented by the $\tau_{visc,max}$ term in Equation (7.5) and removed from the compensation as it depends

on the slip speed (ω_s). The maximum viscous torque is calculated using Equation (4.7) and (7.3) as

$$\tau_{visc,max,clutch} = \frac{N_f \mu_{dyn} \pi \left(R_2^2 - R_1^2\right) r_m^2}{h_{max}} \omega_{R,max} \tag{7.6}$$

$$\tau_{visc,max} = \frac{\tau_{visc,max,clutch}}{\Omega_{clutch}} \tag{7.7}$$

$\tau_{visc,max}$ is the torque acting on the input gear. The ring gear is rotating at maximum when the load is stationary and the motor is running at its nominal speed. The maximum viscous torque is generated at that operation point.
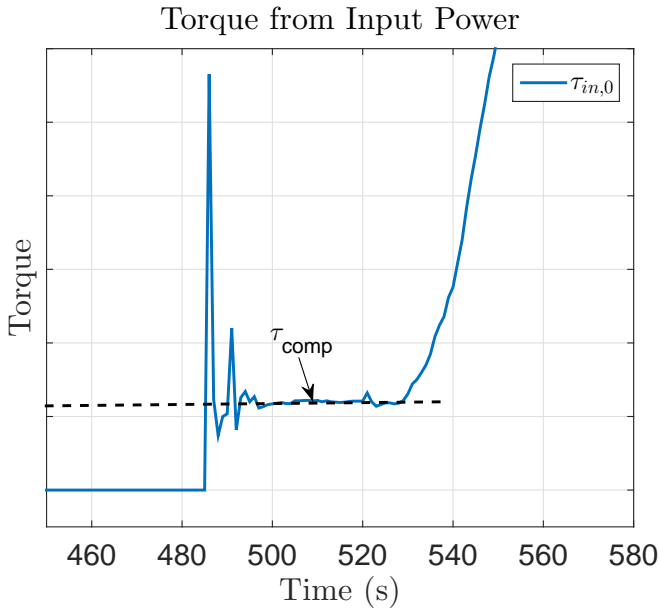
Figure 7.2: Torque from the measured input motor power.

An estimation of the acceleration is made by taking a differential of the measured gear speed ω_R as:

$$\dot{\omega}_R(i) = \frac{\omega_R(i+1) - \omega_R(i)}{T_s} \qquad T_s = 1 \text{ s} \tag{7.8}$$

This is included together with the torque and inertia J_R as the dashed function in Figures 7.7 and 7.8.

7.1.2   Fitting F_{spring}

Adjustments presented in Figure 7.3 are made once to fit the timing of the input power. It is not reasonable to have torque generation not shown in the input power and therefore fitted by adjusting the F_{spring} parameter until the power starts to increase.
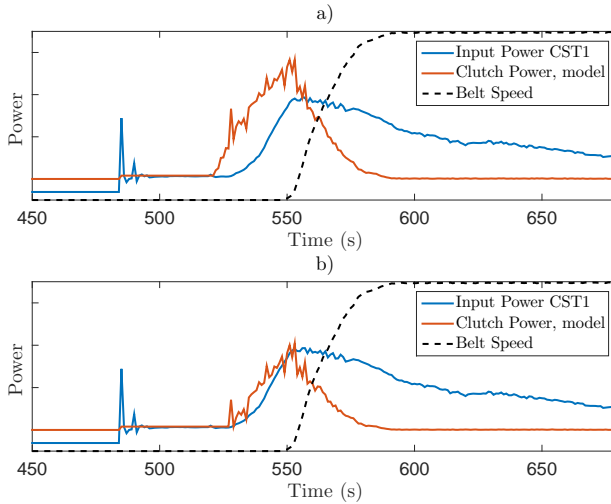
Figure 7.3: *a) Early power generation before the input power increase is not reasonable. b) Adjusting F_{spring} to fit the start time of power increase.*

7.2   Results

The measurements used can be seen in Figure 7.4 and they can be explained as two consecutive engagements. The inserted power differs over the locked periods t∈ [600-1200] and t∈[1400-2600]. This is because the load (mass) changes.

CST-1: Normalized Measurements
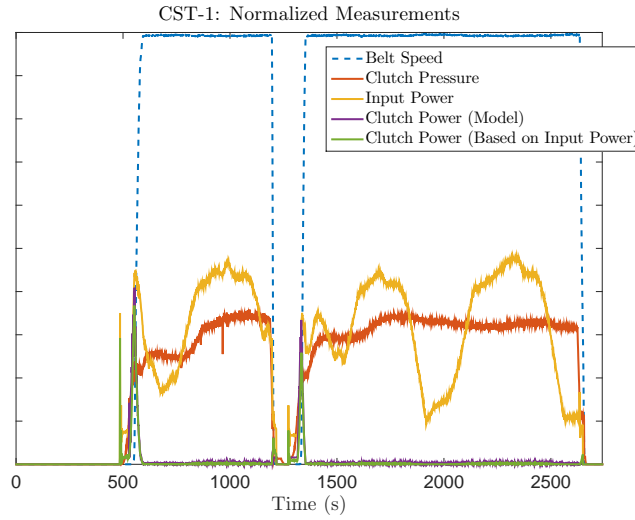
Figure 7.4: Engagement measurements for a CST.

A closer look at the two engagements at t=[500,650] and t=[1300,1400], reveals a slightly large generation of power from the clutch. This is clear in Figures 7.5 and 7.6. The reason for this overshoot is most likely the torque model, as the rotational speed model has less estimated parameters and higher accuracy.
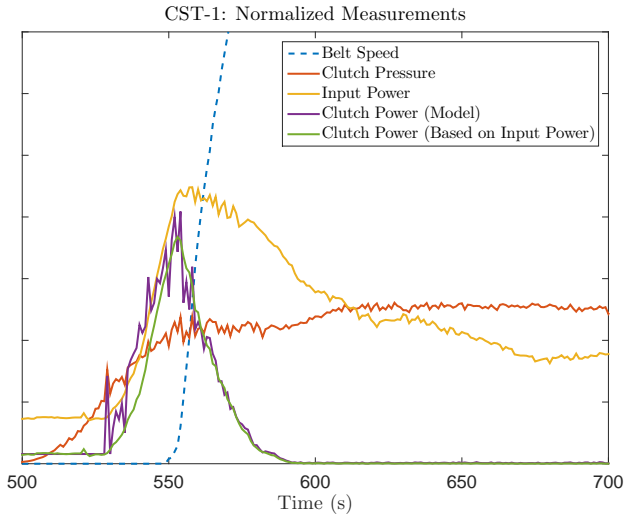
Figure 7.5: *Closer look at the first engagement. The model has a power overshoot in the beginning, seen as the purple curve compared to the linear clutch power from Equation (7.3) in green.*
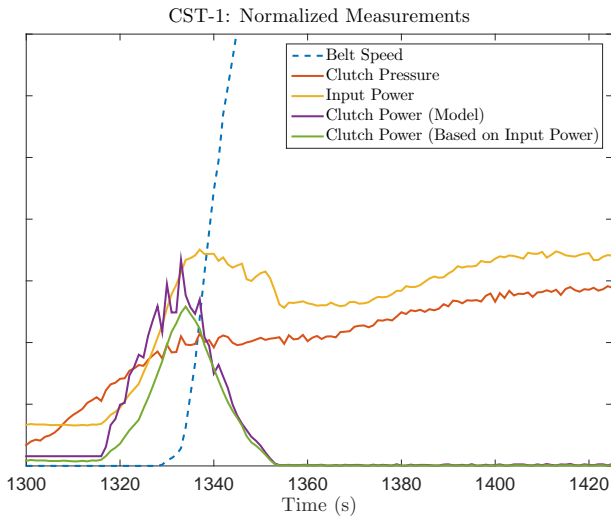
Figure 7.6: *Closer look at the second engagement. Same behavior as the first engagement with a slight early overshoot seen in the clutch power in purple.*

A closer investigation of the generated clutch torque is conducted by comparing the static torque estimated in Equation (7.3) and the clutch torque model using pressure. The input data is fitted for the idle torque before the engagement begins using Equation (7.5).
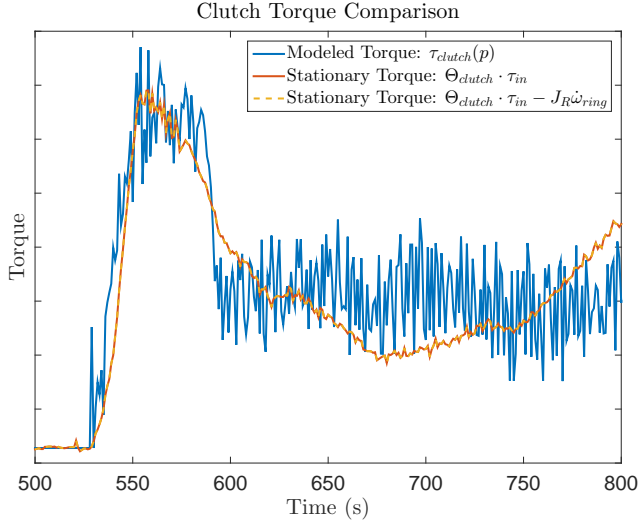
Figure 7.7: Closer look at the first engagement. The pressure model has a power overshoot in the beginning compared to the inserted power model.
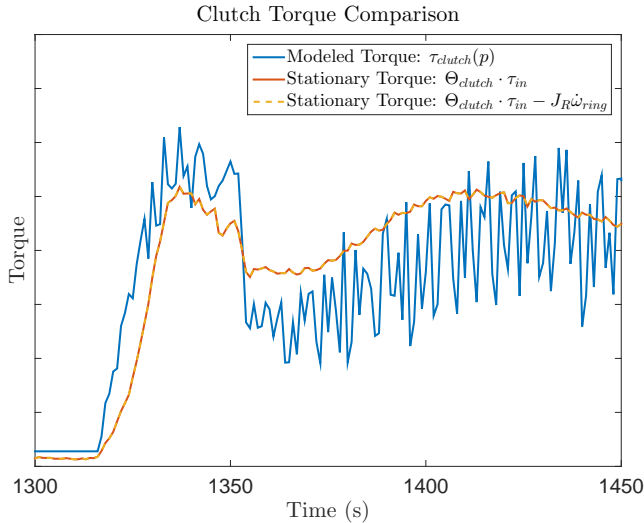
Figure 7.8: Closer look at the second engagement. Overshoot for the pressure model compared to the inserted power model.

In the first engagement in Figure 7.7, the torque has a good fit and according to Equation (3.8) the clutch torque should be larger than the reacting torque to get a negative acceleration of ω_R. The included acceleration from Equation (7.8) is not large enough to have any larger impact on the results of both the engagements. The second engagement in Figure 7.8 has a little larger overshoot over and similar behavior with the stationary torques after t=1350 s.

7.3   Discussion

The torque has an acceptable fit if the F_{spring} parameter is adjusted to measurement data as described in Section 7.1.2. Although it is not measured torque, the comparison can give an idea of the fit. F_{spring} is fitted around 80% larger than the maximum physical parameter although there are presumably other things included in that fitting as well for example friction against the housing and the compression of the oil in the clutch. The result mostly focuses on the generated torque as this is the main part in the heat generation and therefore the thermal behavior of the clutch. Overall there is an overestimation of the clutch torque generated from this model and the reasons for this overshoot can be many things. Some are presented below.

Frictional parameters and model

The friction in this model is modeled from a paper and can be further investigated and fitted to the current application. This can be done using a tribometer and following the same procedures presented in Marklund and Larsson [2008].

Faulty assumption of slow dynamics

The assumption that the clutch is working under constant slip as a limited slip differential can be one of the reasons for the overshoot. The implications would be that the hydrodynamics impacts the torque more than expected. The hydrodynamics are heavily dependent on the clutch compression speed ($\dot{h}$) and it needs to be modeled together with a piston model.

Scalability

The models used in this thesis are all based on relatively small clutches and differentials. The sheer size of the clutch used in the CST or the amount of oil that flows through it can have some implications of the transferred torque.

Further investigation would be necessary to confirm the overall fit of the model, for both the temperature transfer and the generated torque.

8

Conclusions, Reflections and Future Work

8.1 Conclusions

There are several conclusions that can be drawn from this thesis. There are not many articles addressing the high torque - low speed clutch modeling. The result can be interpreted as a indication of how much heat one can expect to be generated in the clutch but the validation is left for later work. The model is implemented and some measurements were done and simulated together with a simulated PLC controller and a model over a conveyor belt. When investigating different measurements and simulations it is seen that in order to minimize the temperature in the clutch and thereby the energy loss it is best to minimize the time spent compressing and building torque to overcome the load. As the load starts to move the CST is a pretty efficient machine and the losses are mostly mechanical.

8.2 Reflections

When the thesis started, a lot of work was spent on compiling a wide base of articles and different models. This was good to get into the reasonable new area for me at least. The approach used, was from a control perspective and the goal was to have a model used as online observer to aid the CST control strategy and also investigate control performance. This might have limited some of the accuracy and behavior of the CST clutch. The result was still acceptable without going too far into the details while keeping the complexity reasonable low.

8.3   Future Work

To expand the model further a suggestion would be to investigate how much the hydrodynamic actually influences the torque. In this thesis hydrodynamics based on compression speed was neglected as explained in Section 4.1.1. The assumption was however based on the much smaller LSD clutch. A larger size might have a bigger impact for the CST application. All the points addressed in Section 7.3 are all subjects for future investigations and there is a need for some measurement projects to secure both the model fit and to get an idea of the scalability of the clutch models. An experimental investigation would also be good to get some data for the HTC function and get a better idea over the real temperature in the clutch. Another usage for the result of this thesis is to implement a temperature observer to limit the peak temperature that the cooling oil is exposed to. As the oil is also used for lubrication and it is shown by Lingesten [2012] that the wear of the oil is accelerated when exposed to higher temperatures.

8.3.1   Experimental Suggestions

In order to validate the model, the following experimental investigations is suggested. It can be divided into three different investigations. friction, compression and heat transfer coefficient.

Friction Parameters

The friction parameter can be obtain through different ways. Either doing a pin-on-disc investigation as described by Marklund and Larsson [2008] or full clutch measurements. Pin-on-disc investigations use a tribometer and a sample of a friction disc. The separator disc materials are often regular steel and the correct oil specified in the user manual should be used. The sample is cut fitted so combined with a suitable weight to create the nominal surface pressure created in the real application. The surface speed depends on the radius and rotational speed of the ring gear. The sample should be fitted with a thermo couple for temperature measurements. At a fixed operating temperature, speed up and let friction brake a rotating disc to a stand still. Repeat for different temperatures to get a good mapping of the friction behavior.
The same procedure can also done with a full clutch setup.

Heat Transfer Coefficient and Compression

The parameters measured is the clutch torque, separator disc temperature, speed, actuator pressure and if possible actuator position. A suggestion of an accurate control of the actuator is presented in Myklebust and Eriksson [2012] though a dry clutch system is used. This can be combined to get measurements to possibly validate a model of the compression rate ($\dot{h}$). A thermo couple mounted in the center of separator disc to get similar position as the temperature model described in this thesis. The measurement procedure to map the HTC parameter over stationary temperature and steps in rotational speed and applied force is similar to Deur et al. [2005], Seo et al. [2015]. For the compression rate it is possible to do step experiments in pressure or clutch piston position.

Appendix

A

Calculations and Matrix Presentation

The calculation results are presented here.

A.1 Kinetic model matrix calculations

The content of the matrix for Ω is as follows:

$$\begin{bmatrix} \dot{\omega}_S \\ \dot{\omega}_C \\ \dot{\omega}_R \\ F \end{bmatrix} = C \cdot \begin{bmatrix} -J_C r_R^2 - J_R r_R^2 - J_R r_S^2 - 2J_R r_R r_S & J_R r_S(r_R + r_S) & J_C r_R r_S \\ -J_R r_S(r_R + r_S) & J_S r_R^2 + J_R r_S^2 & -J_S r_R(r_R + r_S) \\ J_C r_R r_S & J_S r_R(r_R + r_S) & -J_C r_S^2 - J_S r_R^2 - J_S r_S^2 - 2J_S r_R r_S \\ J_C J_R r_S & J_R J_S(r_R + r_S) & J_C J_S r_R \end{bmatrix} \begin{bmatrix} \tau_{sun} \\ \tau_{load} \\ \tau_{clutch} \end{bmatrix}$$

$$C = \frac{1}{J_C J_R r_S^2 + J_C J_S r_R^2 + J_R J_S r_R^2 + J_R J_S r_S^2 + 2J_R J_S r_R r_S}$$

B

Sensitivity Analysis Result Plots
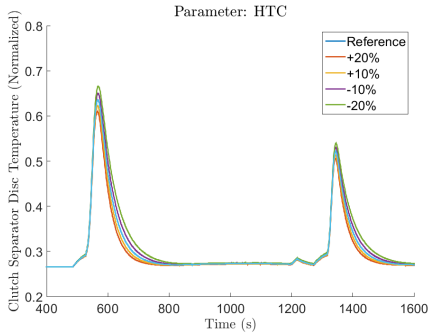
Figure B.1: *Sensitivity analysis for the a constant HTC parameter.*
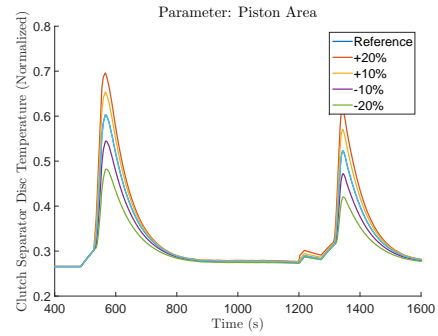
Figure B.2: *Sensitivity analysis for the clutch piston area.*
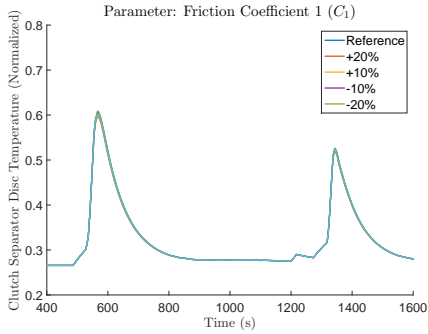
Figure B.3: *Sensitivity analysis for friction coefficient 1.*
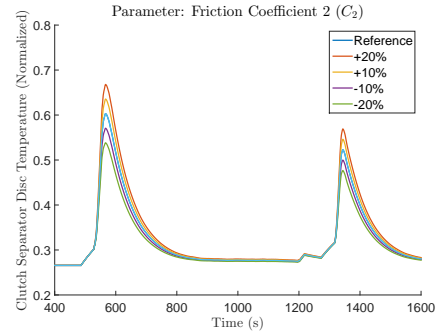
Figure B.4: *Sensitivity analysis for friction coefficient 2.*
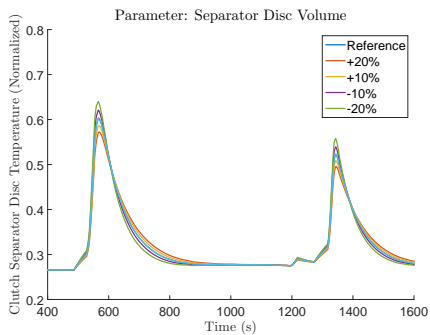
Figure B.5: *Sensitivity analysis for separator plate volume.*
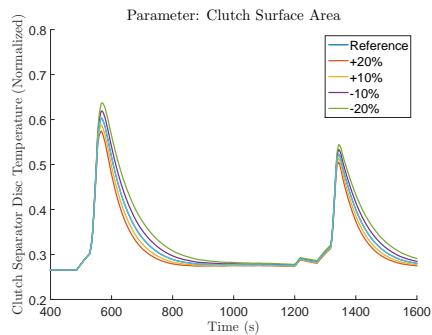
Figure B.6: *Sensitivity analysis for clutch surface area.*
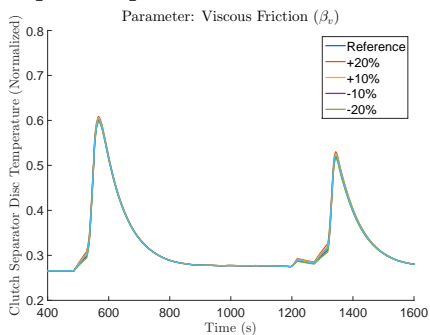
Figure B.7: *Sensitivity analysis for viscous friction parameter.*
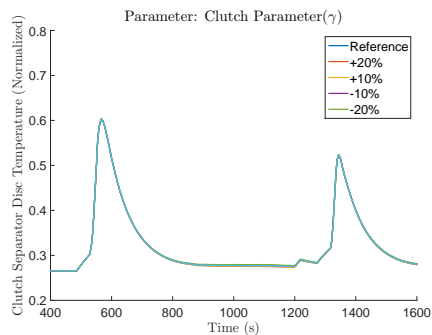
Figure B.8: *Sensitivity analysis clutch parameter γ.*
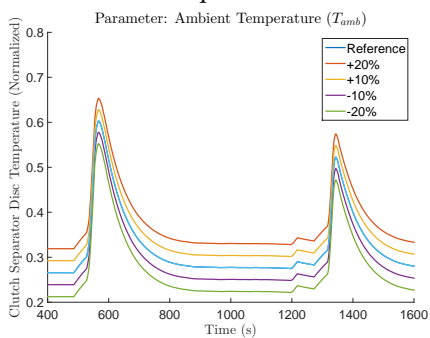
Figure B.9: *Sensitivity analysis for ambient temperature.*

Bibliography

ABB/Baldor-Dodge. Controlled start transmission brochure, year = accessed 2015-06-10,. Cited on pages 6 and 7.

Oday Ibraheem Abdullah and Josef Schlattmann. An investigation of heat generation due to friction using finite element method. Technical report, SAE Technical Paper, 2014. Cited on page 19.

Shushan Bai, Joel Maguire, and Huei Peng. *Dynamic Analysis and Control System Design of Automatic Transmissions*. SAE International, 2013. Cited on pages 11 and 17.

Josko Deur, Josko Petric, Jahan Asgari, and Davor Hrovat. Modeling of wet clutch engagement including a thorough experimental validation. In *SAE Technical Paper*. SAE International, 04 2005. doi: 10.4271/2005-01-0877. URL `http://dx.doi.org/10.4271/2005-01-0877`. Cited on pages 2, 17, 19, and 52.

Vladimir Ivanović, Zvonko Herold, Joško Deur, Matthew Hancock, and Francis Assadian. Experimental characterization of wet clutch friction behaviors including thermal dynamics. *SAE Int. J. Engines*, 2:1211–1220, 04 2009. doi: 10.4271/2009-01-1360. URL `http://dx.doi.org/10.4271/2009-01-1360`. Cited on pages 2, 17, 18, 19, 20, 21, 22, 24, 25, and 33.

Vladimir Ivanović, Joško Deur, Zvonko Herold, Matthew Hancock, and Francis Assadian. Modelling of electromechanically actuated active differential wet-clutch dynamics. *Proceedings of the Institution of Mechanical Engineers, Part D: Journal of Automobile Engineering*, 2011. Cited on page 17.

Han Yu Jin, Xiu Sheng Cheng, and Xiu Feng Song. Rig test and analysis of dynamic engagement process of wet clutch. In *Advanced Materials Research*, volume 945, pages 1461–1464. Trans Tech Publ, 2014. Cited on page 18.

Hisanao Kitabayashi, Chen Yu Li, and Henry Hiraki. Analysis of the various factors affecting drag torque in multiple-plate wet clutches. In *SAE Technical Paper*. SAE International, 05 2003. doi: 10.4271/2003-01-1973. URL `http://dx.doi.org/10.4271/2003-01-1973`. Cited on page 19.

Niklas Lingesten. Wear behavior of wet clutches. 2012. Cited on page 52.

Pär Marklund and Roland Larsson. Wet clutch under limited slip conditions-simplified testing and simulation. *Proceedings of the Institution of Mechanical Engineers, Part J: Journal of Engineering Tribology*, 221(5):545–551, 2007. Cited on pages 2, 17, and 19.

Pär Marklund and Roland Larsson. Wet clutch friction characteristics obtained from simplified pin on disc test. *Tribology International*, 41(9):824–830, 2008. Cited on pages 2, 18, 50, and 52.

Pär Marklund, Rikard Mäki, Roland Larsson, Erik Höglund, M.M. Khonsari, and Joonyoung Jang. Thermal influence on torque transfer of wet clutches in limited slip differential applications. *Tribology International*, 40(5):876 – 884, 2007. ISSN 0301-679X. doi: http://dx.doi.org/10.1016/j.triboint.2006.09. 004. URL http://www.sciencedirect.com/science/article/pii/ S0301679X06003124. Cited on pages 2 and 19.

Andreas Myklebust and Lars Eriksson. Torque model with fast and slow temperature dynamics of a slipping dry clutch. In *Vehicle Power and Propulsion Conference (VPPC), 2012 IEEE*, pages 851–856. IEEE, 2012. Cited on page 52.

Noshir K Romani. A refined soft start technique for long conveyor belts. *SME Annual Meeting & Exhibit, Seattle, WA.*, 2012. Cited on page 1.

Fredrik Roos and Christer Spiegelberg. Relations between size and gear ratio in spur and planetary gear trains. Technical Report 1, KTH, Machine Design (Dept.), 2005. QC 20100816. Uppdaterad från Artikel till Rapport 20100816. Cited on page 13.

Howon Seo, Chunhua Zheng, Wonsik Lim, Suk Won Cha, and Sangchull Han. Temperature prediction model of wet clutch in coupling. In *Vehicle Power and Propulsion Conference (VPPC), 2011 IEEE*, pages 1–4. IEEE, 2011. Cited on page 2.

Howon Seo, Suk Won Cha, Wonsik Lim, and Sangchul Han. Method for estimating temperature of 4wd coupling device wet clutches in severe operating condition. *International Journal of Precision Engineering and Manufacturing*, 16(1):185–190, 2015. Cited on pages 2 and 52.

Sarah Thornton, Gregory M Pietron, Diana Yanakiev, James McCallum, and Anuradha Annaswamy. Hydraulic clutch modeling for automotive control. In *Decision and Control (CDC), 2013 IEEE 52nd Annual Conference on*, pages 2828–2833. IEEE, 2013. Cited on page 2.

Yiqing Yuan, Eysion A Liu, James Hill, and Qian Zou. An improved hydrodynamic model for open wet transmission clutches. *Journal of Fluids Engineering*, 129(3):333–337, 2007. Cited on page 8.